RESEARCH ARTICLE

Hybrid Nanofluid Heat Transfer Adjacent to Vertical Permeable Surface in the Presence of Thermal Boundary Slip

Uzma Ahmad[1,*] **and Kainat Jafri**[1]

[1] Department of Mathematics, Faculty of Science, University of Sargodha, Sargodha 40100, Pakistan

Abstract

The class of fluid known as hybrid nanofluid has numerous engineering applications in the thermal industry. This study is focused on the heat transmission of the hybrid nanofluid adjacent to a vertical permeable surface by incorporating thermal boundary slip. To support this analysis, a mathematical framework has been established, presenting the problem in terms of coupled nonlinear partial differential equations. These equations have been transformed into a system of dimensionless partial differential equations using appropriate dimensionless variables. Furthermore, the finite difference technique has been employed to obtain the appropriate results. The effects of various dimensionless engineering physical parameters related to hybrid nanofluids have been examined in terms of heat transient rate, coefficient of skin friction, velocity, and temperature profiles. The findings are summarized in both graphical and tabular formats. It is keenly observed that, as the numeric values of transpiration parameter (ξ_i) rise, the inclusion of thermal boundary slip leads to an augmentation of velocity and thermal profile at the surface under the effects of both suction and injection. However, an enhancement in the Prandtl number (P_r) results in a decline in velocity profile and an improvement in temperature distribution for both suction and injection.

Keywords: hybrid nanofluid, permeable surface, thermal boundary slip, finite difference technique.

1 Introduction

Heat transfer is the mechanism by which heat is transferred between different mediums or within a single medium, when they are at different temperatures. The means of heat transfer are categorized as: conduction, convection, and thermal radiation. A fluid with enhanced heat transfer characteristics can be devised by combining a base fluid with nanoparticles, named as a nanofluid. The dispersed nanoparticles and the used base fluid create distinctions between different nanofluids. Base fluid refers to the primary fluid in which nanoparticles are dispersed. It serves as a carrier fluid for nanoparticles. Frequently used base fluids are water, oil, ethylene glycol, etc. To get greater and enhanced heat

Submitted: 26 March 2025
Accepted: 07 May 2025
Published: 21 June 2025

Vol. 1, **No.** 1, 2025.
10.62762/CEHT.2025.611372

***Corresponding author:**
✉ Uzma Ahmad
uzma.ahmad@uos.edu.pk

Citation
Ahmad, U., & Jafri, K. (2025). Hybrid Nanofluid Heat Transfer Adjacent to Vertical Permeable Surface in the Presence of Thermal Boundary Slip. *Computational Environmental Heat Transfer*, 1(1), 39–50.

© 2025 by the Authors. Published by Institute of Central Computation and Knowledge. This is an open access article under the CC BY license (https://creativecommons.org/licenses/by/4.0/).

transfer characteristics, we can transform nanofluids into a hybrid nanofluid by dispersing a suitable blend of multiple nanoparticles in the same primary fluid. It's very evident that in industrial and thermal management, nanofluids play a vital role in various fields, including industrial and technological applications. A permeable surface refers to a surface that allows water to penetrate through it. Such a surface facilitates water purification, promotes natural drainage, and refills groundwater. They have wide applications in driveways and sports fields. Thermal boundary slip refers to the odd behavior that occurs at the contact zone of the fluid and rigid surface. In comparison with bulk fluids, molecules exhibit distinct behavior near the boundary. This unusual behavior is visible when the slip length, which controls velocity and temperature gradient at the solid fluid interface, changes. This phenomenon is very essential in nanofluids and microfluids.

Clarke et al. [1] examined free convection for a horizontal porous heated surface. Variable gas properties were observed by assuming the fact that dynamic viscosity and thermal conductivity were relational to temperature. Schlichting et al. [2] analyzed the boundary equations for turbulent and laminar flows. Flow around circular cylinders and stagnation point flow were also observed. Roganov et al. [3] discussed various features and characteristics of turbulent heat transfer at permeable surfaces. The modelling for a relation between pressure and temperature was underscored. Chaudhary et al. [4] employed similarity solutions to solve the model for free convective fluid flow along permeable erect surfaces immersed in porous material. It was observed that solutions were reliant on two dimensionless parameters, namely the mass transfer parameter and power law exponent. A novel class of fluid named as hybrid nanofluid was explored for enhanced heat transfer characteristics by Eastman [5]. It was observed that even a small proportion of nanoparticles in the fluid turned out with better heat transmission characteristics of the fluid. Hussain et al. [6] considered buoyancy-driven heat and mass transport from an upright permeable smooth plate having a non-constant temperature. Four variant approaches were employed to get the numerical solution of governing equations, including the perturbation method, asymptotic solutions, Keller-box method, and local non-similarity approach. The transition of heat transfer from enhancement to reduction for different aspect ratios was examined by Yu et al. [7]. They considered laminar flow for rectangular micro channels and used the integral transform technique to resolve the energy equation. Results were tabulated in terms of local and mean Nusselt numbers. Ali et al. [8] studied laminar free-forced convection flow that arises due to the continuous stretching of the permeable surface. It was observed that the buoyancy force had no impact on the surface due to the reverse correlation between temperature and distance above the surface. The partial slip flow of a Newtonian fluid across a stretchable sheet was considered by Andersson et al. [9]. The numeric values of non-dimensional slip factor, from zero to infinity, were used to control partial slip.

Khanafer et al. [10] examined the augmentation in free convection heat flow by taking into account the nanofluids. The model was developed and solved numerically by employing the Finite volume technique. Later on, Maiga et al. [11] extended it for forced convection heat transient for two different geometries. A slip boundary condition was used by Martin et al. [12] to evaluate laminar flow over a plate. It was observed that slip condition dropped down the global drag force, but two-dimensional effects locally increased the skin friction. With the consideration of partial slip, Ariel et al. [13] interpreted the flow characteristics of elastic-viscous fluid over a stretching membrane. They further discussed their findings about the impact of partial slip on the skin friction coefficient and velocity profile. Berg et al. [14] extended the investigation of fluid behavior in porous medium to the two-phase flow by considering the slip boundary condition. It was further observed that the radius of flow channels determines the enhancement in flux due to slip. Abu-Nada et al. [15] utilized nanofluids to boost the heat transfer in horizontal annuli. Moreover, the effect of nanoparticles, with low and high thermal conductivity, on heat transfer characteristics was observed. Ishak et al. [16] considered a mobile porous flat membrane in a parallel stream to examine transpiration impacts over the flow. By keeping the above conditions in view, a respective model is developed and solved by using the finite difference method. Martin et al. [17] allowed a slip boundary condition over a wedge by considering the modified Falkner-Skan solution for streamline flow. A remarkable decrease in skin friction, velocity, and temperature boundary layer thickness is noticed due to the inclusion of a slip boundary condition. Ishak [18] considered a flat permeable surface whose bottom is heated with the hot fluid

through convection. It was noticed that the thermal transfer rate escalates due to suction. Abu-Nada et al. [19] focused on the impacts of varying thermal conductivity and fluctuating viscosity of nanofluids, -water and CuO-water on free convection heat transfer in enclosures.

Aziz [20] took into consideration a uniformly heated flat plate under the influence of thermal slip flow. It was observed that the slip parameter relates directly to slip velocity and inversely to wall shear stress. Temperature variant viscosity and thermal conductivity of micro polar fluid for an inclined permeable wall were investigated by Rahman et al. [21]. It was noted that an increase in the thermal conductivity parameter upturned the velocity and temperature of the boundary layer. Impact of thermal radiation on a magnetically influenced upstanding plate was investigated by Ashraf et al. [22] for free-forced convection. Effects of dimensionless parameters were observed graphically and in tabular form against the skin friction coefficient and the transpiration parameter. Buoyancy-driven flow in a cavity, whose lateral walls were thermally active, was computationally studied by Sheikhzadeh et al. [23]. The enclosure was occupied by Cu water nanofluids. It was concluded that there is an escalation in the average Nusselt number with the rise in Rayleigh number and volume fraction of dispersed nanoparticles. Accounting for the effects of Brownian motion and thermophoresis, Khan et al. [24] numerically explored the buoyancy-driven flow over an erect plate having constant heat flux. The transport mass and energy equations were further analyzed by using similarity transformations. Subjected to a transverse magnetic force field, Su et al. [25] investigated Falkner-Skan flow in the boundary layer region above a permeable plate. A comparison was made between the approximate and numerical solutions, and found that they were in good agreement. Suresh et al. [26] examined the influence of water-based hybrid nanofluid in heat transfer for uniformly heated circular tubes. It was perceived that an enhancement in the convective heat transfer coefficient causes an increase in the Reynolds number. Under the action of radiant energy and temperature-dependent heat transmission, Cortell [27] examined heat transfer characteristics for an incompressible fluid above a stretching penetrable interface within a porous material. Moreover, the consequences of Pr, fluctuating thermal conductivity, permeability, and thermal radiation on the rate of heat transfer were plotted graphically and also presented in tabular form. Alvarino et al. [28] explored the implications of molecular and thermal diffusion in the entrance area of a tube for convective heat transfer in hybrid nanofluids. Ashraf et al. [29] studied the cumulative impact of radiation-conduction and hydro magnetics for electrically conducting fluid across a magnetized perpendicular permeable plate. Finite difference technique was adopted to compute the numeric solution of equations. Huminic and Huminic [30] summarized significant work of many researchers related to the effectiveness of nanofluids in the augmentation of convectional heat transfer in heat exchangers. Heat conduction and viscosity of nanofluids were also discoursed theoretically and experimentally. Noghrehabadi et al. [31] reported the impact of partial slip over a stretching surface for boundary layer flow influenced with nanoparticles. A strong impact of the slip parameter over the flow velocity and shear stress of the stretching sheet was observed. Ibrahim et al. [32] explored boundary layer flow for a stretching permeable sheet. An enhancement in sheet temperature was observed due to an increase in values of the Echert number. Runge Runge-Kutta approach was applied to numerically integrate the equations. Labib et al. [33] inspected the influence of conventional fluids on convective heat transfer mixed with nanoparticles, by using two distinct base fluids. It was noticed that ethylene glycol proved more beneficial for enhanced heat transfer as compared to water. Four distinct nanoparticles along with water as carrier the fluid were considered by Abolbashari et al. [34] to examine MHD flow for stretching a permeable surface. Homotopy perturbation method was implemented to resolve fundamental equations. Also, the impact of thermophysical parameters was observed graphically. The benefits of using porous medium impacted by nanofluid were discussed by Mahdi et al. [35]. It was noted that as compared to conventional fins, the dissipation area of porous medium was much greater, which resulted in the amplification of heat transfer characteristics.

In view of the limited understanding of nanofluid heat transfer mechanisms, Sarkar et al. [36] apprehend the advantages and suitable applications of hybrid nanofluids in heat transient enhancement and pressure gradient attributes, respectively. Later, Sidik et al. [37] apprehend the production of hybrid nanoparticles and hybrid nanofluid, and also their effectiveness in thermal energy transient. The future challenges related to the application of hybrid nanofluids have

also been discussed. Aluminum nitride nanoparticles were distributed in ethylene glycol, which served as a base fluid, by Hussein et al. [38] to escalate the heat transient mechanism within a dual-tube heat exchanger. It was found that the thermal performance of the heat exchanger was more promising for composite nanofluids in relation to traditional fluids. Kasaeian et al. [39] reported thermal transport traits of nanofluid for porous medium. It was observed that the combined effect of porous media and nanofluid augmented heat transfer in a heat exchanger. The problem of MHD flow for permeable walls of a channel was researched by Fakour et al. [40]. The least squares method was executed to solve the resulted differential equations of higher order. The outcomes were contrasted with the one already presented in the literature to examine their validity. Sundar et al. [41] pointed out the drawbacks of using a hybrid nanofluid. It was explored that the higher the heat transfer rate, the higher the viscosity of the fluid. The impact of platinum hybrid nanofluid over heat flux was observed by Yarmand et al. [42]. It was witnessed that the elevation in the Nusselt number relied upon the values of the Reynolds number. Bhattad et al. [43] numerically and experimentally explored the impact of hybrid nanofluid on pressure variance and heat transfer efficiency of a plate heat exchanger. Velocity and thermal boundary layer profiles have been established for base fluid, nanofluids, and nanostructured fluid. Minea et al. [44] compared traditional fluids with hybrid nanofluids in terms of heat transfer characteristics. It was reported that a synergistic effect, leading to long-term stability, can be obtained by fusion of appropriate nanoparticles in a base fluid.

The role of nanofluid and hybrid nanofluid in thermal conductivity for the shrinking sheet was observed by Aly et al. [45]. In relation to nanofluid, hybrid nanofluid proved more fruitful for heat transfer in the case of a shrinking sheet. Kumar et al. [46] investigated the impact of nonlinear radiant energy and a continuously varying heat source and sink on a micropolar fluid flow above a stretching surface by considering a second-order slip condition. Appropriate similarity variables were used to transform PDEs into ODEs. It was predicted that the velocity distribution would be strengthened and the temperature distribution would be reduced due to second-order slip. Sidik et al. [47] assessed the methods of synthesizing hybrid nanofluids and the factors affecting their performance. It was further predicted that hybrid nanofluids work very effectively as a substitute for the convective coolants working at higher temperatures. In [48], the existing facts about hybrid nanofluids and the challenges and difficulties faced by the fresh researchers were discussed in detail. It was further advised that, regardless of the attractive and effective characteristics of hybrid nanofluids, a lot of devotion is needed in the development, implementation, and stability of models, helpful in simulating the thermodynamic pattern and heat transient features. Effectiveness of the Lorentz force and irregular viscosity in the augmentation of heat transfer, with the influence of nanoparticles-based hybrid fluid, was considered by Manjunatha et al. [49]. Ashraf et al. [50] studied boundary layer flow of nanofluids at distinct positions on a sphere under free convection conditions. It was observed that the concentration of nanoparticles was minimum at site , but maximum at respectively. Shafiq et al. [51] examined three-dimensional rotating frame influenced with thermal boundary slip for nanofluid flow. The prominent feature of this work was Arrhenius activation energy. It was observed that elevation in stretching values resulted in a reduction of fluid velocity.

A permeable elastic sheet was considered by Roy et al. [52] to investigate thermal aspects of a second-grade nanofluid mixture. It was seen that the suction parameter is related directly to fluid velocity and inversely to temperature. Waini et al. [53] studied MHD flow over a shrinking permeable wedge for a hybrid nanofluid. MATLAB was leveraged to optimize the primary equations numerically. It was concluded that an increase in the radiation parameter caused a decrease in the rate of heat transfer. Jeelani et al. [54] examined non non-Newtonian Maxwell model in which ethylene glycol served as a base fluid with the dispersion of alumina and copper nanoparticles to investigate heat transfer enhancement. A numerical solver, bvp4c, is utilized to obtain a solution of the underlying equations. Bhattad et al. [55] reviewed preparation techniques and implications of mono-nanofluid and nanofluid mixtures. Their characteristics as a working fluid were also underscored.

In view of previous studies, this dissertation aims at the enrichment of mixed convective heat transfer in the close neighborhood of a permeable vertical surface with the inclusion of thermal boundary slip. The variations in the flow structure, including velocity and thermal boundary layer profiles, will be analyzed.

2 Mathematical Simulation and Fundamental Equations

A dual dimensional steady, viscous flow of hybrid nanofluid alongside a permeable vertical plate is considered in Figure 1. The surface lies in direction while -axis is at right angle to it. The thermo-physical specifications of the fluid are considered invariable, where the viscosity and density are considered to be of the hybrid nanofluid. To merge the impact of thermal boundary slip, adjustments are made in the respective boundary conditions of the model.

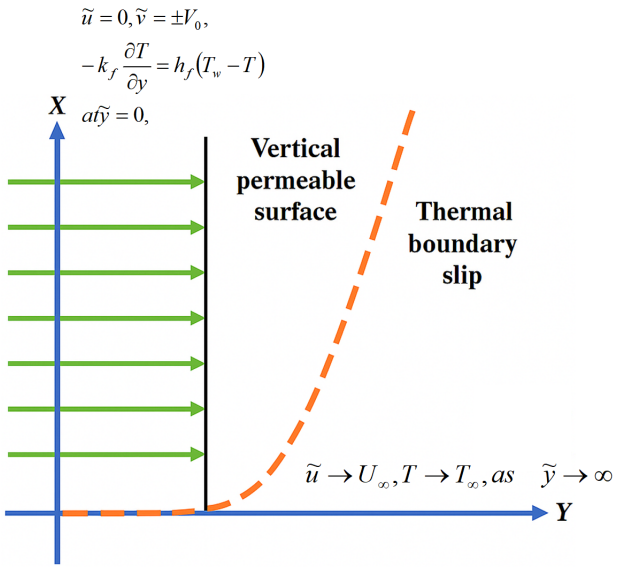

Figure 1. Vertical permeable plate with thermal boundary slip.

In reliance on the above premises and by following [29] and [54], the boundary layer coupled mass, momentum, and energy equations are formulated as:

$$\frac{\partial \tilde{u}}{\partial \tilde{x}} + \frac{\partial \tilde{v}}{\partial \tilde{y}} = 0 \tag{1}$$

$$\tilde{u}\frac{\partial \tilde{u}}{\partial \tilde{x}} + \tilde{v}\frac{\partial \tilde{u}}{\partial \tilde{y}} = \frac{\mu_{\text{hnf}}}{\rho_{\text{hnf}}}\frac{\partial^2 \tilde{u}}{\partial \tilde{y}^2} + g\frac{(\rho\beta_T)_{\text{hnf}}}{\rho_{\text{hnf}}}(T - T_\infty) \tag{2}$$

$$(\rho C_p)_{\text{hnf}}\left(\tilde{u}\frac{\partial T}{\partial x} + \tilde{v}\frac{\partial T}{\partial y}\right) = K_{\text{hnf}}\frac{\partial^2 T}{\partial y^2} \tag{3}$$

where $\tilde{u}$ and $\tilde{v}$ are the horizontal and normal components of velocity, respectively. μ_{hnf}, ρ_{hnf}, $(\rho\beta_T)_{\text{hnf}}$, K_{hnf}, $(\rho C_p)_{\text{hnf}}$ indicate fluid's consistency, fluid's concentration, thermal expansion coefficient, thermal transport coefficient, and volumetric heat capacity of hybrid nanofluid, respectively. T refers to the temperature of the fluid.

The associated boundary conditions (by following [51]) are:

$$\begin{aligned} &\tilde{u}=0, \quad \tilde{v}=\pm V_0, \quad -K_f\frac{\partial T}{\partial y} = h_f(T_w - T), \quad \text{at } \tilde{y}=0; \\ &\tilde{u} \to U_\infty, \quad T \to T_\infty, \quad \text{as } \tilde{y} \to \infty \end{aligned} \tag{4}$$

where k_f is the thermal conductivity of the fluid and h_f is the heat transfer coefficient.

3 Dimensional Analysis

Dimensional analysis is a process employed on equations to combine distinct physical quantities in such a way that the dimensions of the quantities get canceled out. The originated unit-less quantities help to describe the behavior of fluid independent of units. It is used to analyze the system behavior and explore the dominant physical controlling factor of the system.

To obtain dimensionless boundary layer equations and respective interface conditions, we are going to introduce the following scale-invariant parameters.

$$\begin{aligned} u = \frac{\tilde{u}}{U_\infty}, \quad v = \frac{\tilde{v}}{U_\infty}\text{Re}^{\frac{1}{2}}, \quad \theta = \frac{T - T_\infty}{T_w - T_\infty}, \\ y = \frac{\tilde{y}}{L}\text{Re}^{\frac{1}{2}}, \quad x = \frac{\tilde{x}}{L} \end{aligned} \tag{5}$$

By substituting (5) in equations (1) – (4), the obtained dimensionless model is stated as

$$\frac{\partial u}{\partial x} + \frac{\partial v}{\partial y} = 0 \tag{6}$$

$$u\frac{\partial u}{\partial x} + v\frac{\partial v}{\partial y} = \frac{\mu_{\text{hnf}}}{\mu_f}\cdot\frac{\rho_f}{\rho_{\text{hnf}}}\frac{\partial^2 u}{\partial y^2} + \pm\lambda\frac{(\rho\beta_T)_{\text{hnf}}}{\rho_{\text{hnf}}}\cdot\frac{\rho_f}{(\rho\beta_T)_f}\theta \tag{7}$$

$$u\frac{\partial \theta}{\partial x} + v\frac{\partial \theta}{\partial y} = \frac{1}{\text{Pr}}\cdot\frac{k_{\text{hnf}}}{k_f}\cdot\frac{(\rho C_p)_f}{(\rho C_p)_{\text{hnf}}}\cdot\frac{\partial^2 \theta}{\partial y^2} \tag{8}$$

where u and v correspond to the normalized velocity components along x and y directions, respectively. Moreover, θ, λ, and Pr represent the non-dimensional fluid temperature, mixed convection parameter, and Prandtl number, respectively.

The respective dimensionless boundary conditions are given as:

$$\begin{aligned} &u=0, \quad v=S_{L_1}, \quad \theta' = -S_{L_2}(1-\theta) \quad \text{at } y=0; \\ &u \to 1, \quad \theta \to 0, \quad \text{as } y \to \infty. \end{aligned} \tag{9}$$

where $S_{L_1} = \pm\frac{V_o}{U_\infty}Re^{1/2}$ is transpiration parameter and $S_{L_2} = Re^{-1/2}L\frac{h_f}{k_f}$ is thermal slip parameter.

4 Solution Technique

The finite difference method is a numerical approach employed to get the solution of differential equations. It is an approximation technique centered on discretization. It helps to simplify problems, which facilitates effective handling of complex geometries.

To employ this technique, primarily, the primitive variables are introduced.

4.1 Primitive Variable Formulation

For convenient integration of the obtained dimensionless model, the following parameters are introduced:

$$u = U(\xi, Y), \quad v = x^{-1/2}\left(V(\xi, Y) \pm \xi\right), \quad Y = x^{-1/2}y,$$
$$\xi = S_{L_1}x^{-1/2}, \quad \theta = \bar{\theta}(\xi, Y), \quad x = X. \tag{10}$$

By substituting (10) in boundary layer equations (6) – (8), the mass conservation, energy, and motion equations are transformed into:

$$-\frac{\xi}{2}\frac{\partial U}{\partial \xi} - \frac{1}{2}Y\frac{\partial U}{\partial Y} + \frac{\partial V}{\partial Y} = 0 \tag{11}$$

$$-U\frac{\xi}{2}\frac{\partial U}{\partial \xi} + \left(V - \frac{1}{2}YU \pm \xi\right)\frac{\partial U}{\partial Y} = \frac{\mu_{\text{hnf}}}{\mu_f}\cdot\frac{\rho_f}{\rho_{\text{hnf}}}\cdot\frac{\partial^2 U}{\partial Y^2} \pm \lambda X\cdot\frac{(\varphi\beta T)_{\text{hnf}}}{(\varphi\beta T)_f}\cdot\frac{\rho_{\text{hnf}}}{\rho_f}\,\bar{\theta} \tag{12}$$

$$-U\frac{\xi}{2}\frac{\partial \bar{\theta}}{\partial \xi} + \left(V - \frac{1}{2}YU \pm \xi\right)\frac{\partial \bar{\theta}}{\partial Y} = \frac{1}{Pr}\cdot\frac{\left(\frac{k_{\text{hnf}}}{k_f}\right)}{\left(\frac{(\rho c_p)_{\text{hnf}}}{(\rho c_p)_f}\right)}\cdot\frac{\partial^2 \bar{\theta}}{\partial Y^2} \tag{13}$$

The transformed boundary conditions can be written as:

$$U(\xi, 0) = 0, \quad V(\xi, 0) = 0, \quad \bar{\theta}'(\xi, 0) = -S_{L_2}x^{1/2}(1 - \bar{\theta})$$
$$U(\xi, \infty) \to 1, \quad \bar{\theta}(\xi, \infty) \to \infty \tag{1}$$

4.2 Discretization

With the help of following central difference and backward difference along y and x direction respectively, we will discretize the equations (11) – (13)

$$\begin{aligned}
\frac{\partial U}{\partial \xi} &= \frac{U_{i,j} - U_{i,j+1}}{\Delta\xi} \\
\frac{\partial U}{\partial Y} &= \frac{U_{i+1,j} - U_{i-1,j}}{2\Delta Y} \\
\frac{\partial V}{\partial Y} &= \frac{V_{i+1,j} - V_{i-1,j}}{2\Delta Y} \\
\frac{\partial^2 U}{\partial Y^2} &= \frac{U_{i+1,j} - 2U_{i,j} + U_{i-1,j}}{\Delta Y^2}
\end{aligned} \tag{15}$$

Similarly for θ,

$$\begin{aligned}
\frac{\partial \bar{\theta}}{\partial \xi} &= \frac{\bar{\theta}_{i,j} - \bar{\theta}_{i,j+1}}{\Delta\xi} \\
\frac{\partial \bar{\theta}}{\partial Y} &= \frac{\bar{\theta}_{i+1,j} - \bar{\theta}_{i-1,j}}{2\Delta Y} \\
\frac{\partial^2 \bar{\theta}}{\partial Y^2} &= \frac{\bar{\theta}_{i+1,j} - 2\bar{\theta}_{i,j} + \bar{\theta}_{i-1,j}}{\Delta Y^2}
\end{aligned} \tag{16}$$

By using the above equations (15) and (16) and simplifying the terms, we get the following velocity component from the continuity equation, which can be used to determine the velocity of the fluid.

$$V_{i+1,j} = V_{i-1,j} + \xi_i\frac{\Delta Y}{\Delta\xi}\left(U_{i,j} - U_{i,j+1}\right) - \frac{Y_j}{2}\left(U_{i+1,j} - U_{i-1,j}\right) \tag{17}$$

The discretized version of the momentum transport equation is

$$A_1U_{i+1,j} - B_1U_{i,j} + C_1U_{i-1,j} = D_1 \tag{18}$$

where

$$\begin{aligned}
A_1 &= \frac{\mu_{\text{hnf}}}{\mu_f}\cdot\frac{\rho_f}{\rho_{\text{hnf}}}\left(-\left(V_{i,j} - \frac{Y_j}{2}U_{i,j} \pm \xi_i\right)\frac{\Delta Y}{2}\right), \\
B_1 &= 2\cdot\frac{\mu_{\text{hnf}}}{\mu_f}\cdot\frac{\rho_f}{\rho_{\text{hnf}}} - \frac{\xi_i\Delta Y^2}{2\Delta\xi}U_{i,j}, \\
C_1 &= \frac{\mu_{\text{hnf}}}{\mu_f}\cdot\frac{\rho_f}{\rho_{\text{hnf}}}\left(\left(V_{i,j} - \frac{Y_j}{2}U_{i,j} \pm \xi_i\right)\frac{\Delta Y}{2}\right), \\
D_1 &= \frac{\xi_i\Delta Y^2}{2\Delta\xi}U_{i,j}U_{i,j+1} \pm \lambda X\cdot\frac{(\varphi\beta T)_{\text{hnf}}}{(\varphi\beta T)_f}\cdot\frac{\rho_{\text{hnf}}}{\rho_f}\bar{\theta}_{i,j}.
\end{aligned} \tag{19}$$

And the discretized representation of the energy balance equation is:

$$A_2\,\bar{\theta}_{i+1,j} - B_2\,\bar{\theta}_{i,j} + C_2\,\bar{\theta}_{i-1,j} = D_{2,\psi} \tag{20}$$

where,

$$A_2 = \frac{1}{\mathrm{Pr}} \frac{\frac{k_{\mathrm{hnf}}}{k_f}}{(\rho C_p)_{\mathrm{hnf}} / (\rho C_p)_f} - \left(V_{i,j} - \frac{Y_j}{2} U_{i,j} \pm \xi_i \right) \frac{\Delta Y}{2},$$
$$B_2 = \frac{2}{\mathrm{Pr}} \frac{\frac{k_{\mathrm{hnf}}}{k_f}}{(\rho C_p)_{\mathrm{hnf}} / (\rho C_p)_f} - \frac{\xi_i \, \Delta Y^2}{2 \, \Delta \xi} U_{i,j},$$
$$C_2 = \frac{1}{\mathrm{Pr}} \frac{\frac{k_{\mathrm{hnf}}}{k_f}}{(\rho C_p)_{\mathrm{hnf}} / (\rho C_p)_f} + \left(V_{i,j} - \frac{Y_j}{2} U_{i,j} \pm \xi_i \right) \frac{\Delta Y}{2},$$
$$D_2 = -\frac{\xi_i \, \Delta Y^2}{2 \, \Delta \xi} U_{i,j} \, \overline{\theta}_{i,j+1} \tag{21}$$

The discretized boundary conditions are:

$$U_{i,j} = 0, \quad V_{i,j} = 0, \quad \frac{\overline{\theta}_{i+1,j} - \overline{\theta}_{i-1,j}}{2\Delta Y} = -S_{L_2} \left(1 - \overline{\theta}_{i,j} \right) \quad \text{at } Y_j = 0$$
$$U_{i,j} \to 1, \quad \overline{\theta}_{i,j} \to 0 \quad \text{as } Y_j \to \infty \tag{22}$$

The values of physical properties of hybrid nanofluid used in above equations are stated (by following [54]) as:

$$\frac{k_{hnf}}{k_f} = \frac{(p-1)k_f + k_{r2} - (p-1)\Phi_2(k_{bf} - k_{r2})}{(p-1)k_{bf} + k_{r2} + \Phi_2(k_{bf} - k_{r2})}$$
$$\frac{k_{bf}}{k_f} = \frac{(p-1)k_f + k_{r2} - (p-1)\Phi_2(k_f - k_{r2})}{(p-1)k_f + k_{r1} + \Phi_1(k_f - k_{r1})}$$

$$(\rho C_p)_{hnf} = \Phi_1 (\rho C_p)_{r1} + \Phi_2 (\rho C_p)_{r2} + (1 - \Phi_2) \left[1 - \Phi_1 (\rho C_p)_f \right]$$

$$\rho_{hnf} = (1 - \Phi_2) \left[1 - \Phi_1 \rho_f + \Phi_1 \rho_{r1} \right] + \Phi_2 \rho_{r2}$$

$$\frac{\mu_{hnf}}{\mu_f} = \frac{1}{(1 - \Phi_1)^{2.5} (1 - \Phi_2)^{2.5}}$$

$$(\rho \beta_T)_{hnf} = \Phi_1 (\rho \beta_T)_{r1} + \Phi_2 (\rho \beta_T)_{r2} + (1 - \Phi_2) \left[1 - \Phi_1 (\rho \beta_T)_f \right]$$

where Φ_1 and Φ_2 represent the volume fractions of solid nanoparticles, and r_1 and r_2 denote the thermophysical characteristics of two different types of nanoparticles.

Table 1. Properties of hybrid nano fluids taken in this study.

Thermophysical Properties	**Base fluid (air)**	**Al_2O_3**	**Cu**
ρ (Kg/m^3)	1.225	3970.0	8933
C_p (JKg^{-1}K^{-1})	1007	765.0	385.0
k (Wm^{-1}K^{-1})	0.0255	40.0	400.0

Table 2. Numeric solution of heat transfer rate and skin friction coefficient for a diverse range of Prandtl numbers Pr.

Pr	Skin friction	Heat transfer rate
0.1	31.75944	0.34833
0.71	22.4168	0.73371
3.0	16.78128	1.16082
5.0	15.06431	1.34858
7.0	14.00757	1.48491
10.0	12.94953	1.64171

Table 3. Numeric solution of heat transfer rate and skin friction coefficient for a diverse range of transpiration parameter ξ_i.

ξ_i	Skin friction	Heat transfer rate
0.01	0.40151	0.80025
0.03	0.41002	0.80106
0.05	0.41094	0.80157
0.07	0.41171	0.80295
0.09	0.41221	0.80302
0.10	0.41260	0.80309

5 Data Analysis and Interpretation

This portion illustrates the impact of the dimensionless parameter Prandtl number (Pr) and the transpiration parameter (ξ_i) on the velocity and temperature profiles. This parametric analysis of velocity and temperature facilitates a better understanding of the fluid pattern. The relevant physical properties are summarized in Table 1.

Table 2 depicts the impact of Pr on the frictional drag force C_f and the rate of heat exchange. It is observed from the table that a rise in the magnitude of the Prandtl number decays the frictional resistance. Since a high value of the Prandtl number increases the thickness of the fluid, which decelerates the flowing fluid, leading to the enhancement in the skin friction coefficient C_f. However, this effect of viscosity is encountered by the inclusion of thermal boundary slip. The velocity of the fluid drops due to thermal boundary slip, which in turn reduces the magnitude of skin friction. In the opposite vein, the higher the value of the Prandtl number, the higher is the rate of heat transfer. Since the inclusion of thermal boundary slip decreases the thickness of the thermal boundary layer and develops a temperature gradient in proximity to the surface, it leads to improved heat flux. For $\mathrm{Pr} < 1$, fluid's viscosity is dominated by thermal diffusivity, which elevates heat flux by reducing the frictional force of the fluid.

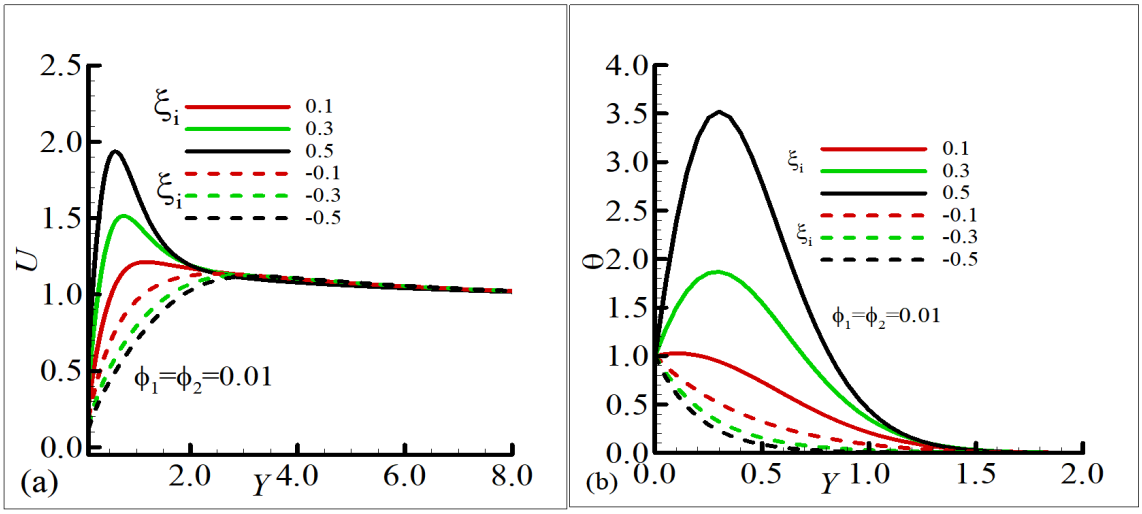

Figure 2. Graphical illustration for (a) velocity U and (b) temperature $\overline{\theta}$ for a diverse range of transpiration parameter $\xi_i = 0.1,\ 0.3,\ 0.5,\ -0.1,\ -0.3,\ -0.5$ and $\lambda = 10.0$.

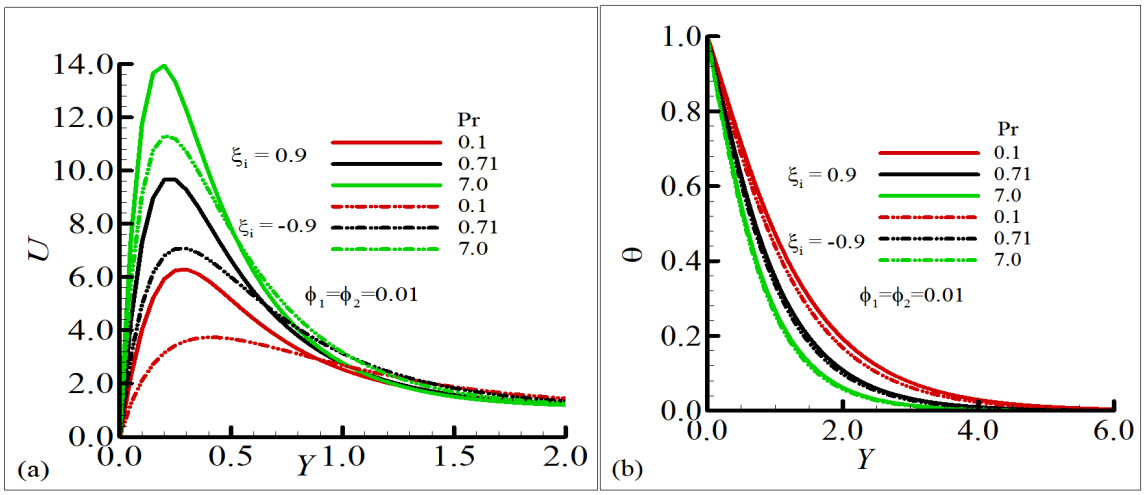

Figure 3. Graphical illustration for (a) velocity U and (b) temperature $\overline{\theta}$ against numerous values of Prandtl number $\mathrm{Pr} = 0.1,\ 0.71,\ 7.0$ and $\lambda = 10.0$.

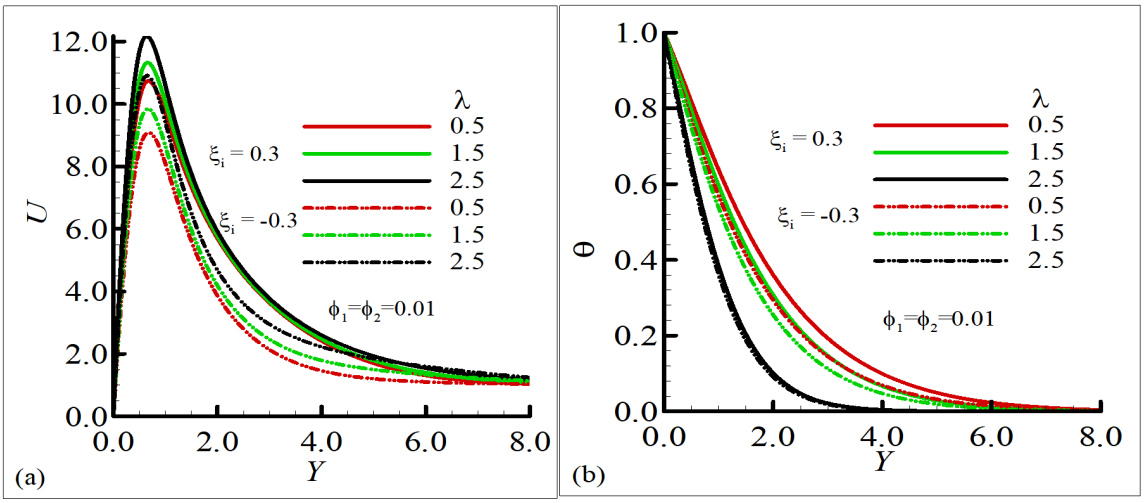

Figure 4. Graphical illustration for (a) velocity U and (b) temperature $\overline{\theta}$ for distinct magnitudes of mixed convection parameter $\lambda = 0.2,\ 0.4,\ 0.6,\ 0.8$ and $\mathrm{Pr} = 7.0$.

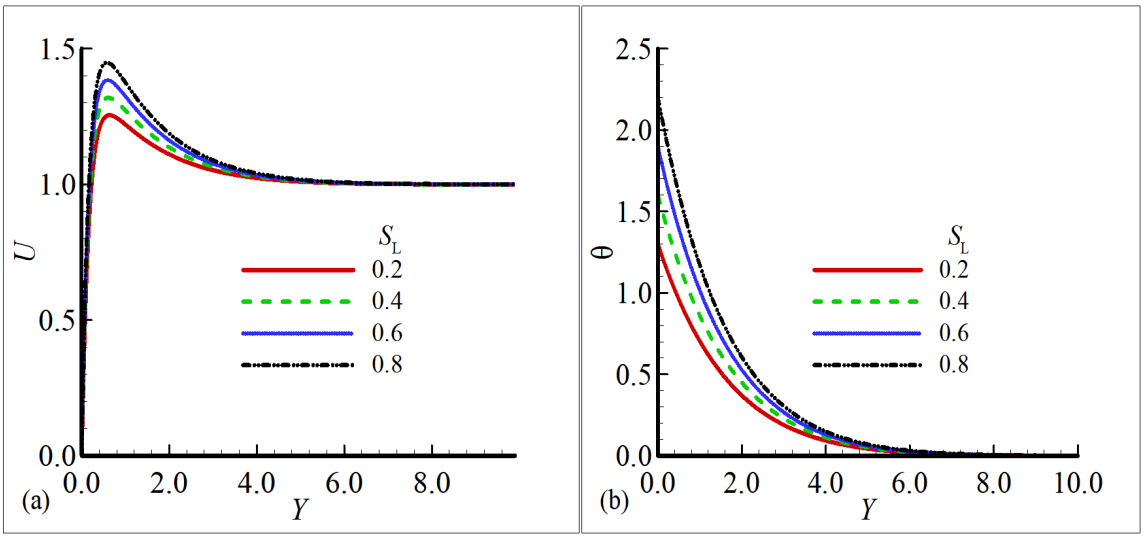

Figure 5. Graphical illustration for (a) velocity U and (b) temperature $\overline{\theta}$ for a diverse range of slip parameter $S_L = 0.2,\ 0.4,\ 0.6,\ 0.8$ and $\mathrm{Pr} = 7.0$.

The impact of the transpiration parameter against skin friction coefficient and thermal flux can be observed from Table 3. It is noted that the transpiration parameter relates directly to the frictional factor and heat transmission rate. Due to the increased value of the transpiration parameter and inclusion of thermal boundary slip, permeability improves. This improved permeability of the surface helps the fluid to get more stabilized and facilitates easy fluid flow through the surface, resulting in enhanced heat transmission characteristics of the fluid. Also, suction reduces the boundary layer thickness of fluid, facilitating more contact between the surface and the flowing fluid. This enhanced contact increases the skin friction coefficient.

Figure 2 portrays how the transpiration parameter ξ_i influences the fluid's velocity U and temperature distribution θ, revealing that with thermal boundary slip considered, suction enhances both velocity and temperature at the surface, while maintaining a constant profile away from it. This occurs because suction is enhanced by the incorporation of thermal slip condition, which reduces the boundary layer thickness, facilitates smoother flow, and improves thermal distribution. In the same manner, increasing values of injection accelerate the fluid and temperature of the fluid due to the significant presence of thermal boundary slip.

Figure 3 characterize the impact of Prandtl number Pr in opposition to fluid velocity and temperature where $\lambda = 10.0$ and $\xi_i = 0.9, -0.9$. It illustrates that for both suction and injection, an elevation in the numeric data of Pr results in the rise of velocity of fluid and a downfall of temperature adjacent to the surface. It shows that for distinct values of Prandtl number, different fluids (water, air, and oil) behave in a similar way for suction and injection.

The impact of mixed convection parameter λ on the temperature and velocity of the fluid is depicted by Figure 4. It is witnessed that elevated values of the mixed convection variable λ boost the velocity and reduce the temperature of the fluid. Since, for higher values of λ, buoyancy flow dominates the forced flow, causing an increase in fluid velocity, and a uniform temperature distribution reduces the temperature of the fluid.

It is observed from Figure 5 that augmentation in slip parameter S_L lessens the boundary layer thickness by improving permeability, which permits fluid to flow faster. As a result, it increases the velocity of the fluid. Since a high value of the slip parameter facilitates fluid flow, it also results in effective thermal characteristics of the fluid.

6 Conclusion

The above study underscores the characteristics of heat transfer for hybrid nanofluid adjacent to a vertical permeable surface influenced by thermal boundary slip. It highlights the impacts of Prandtl number (Pr) and transpiration parameter (ξ_i) against the rate of heat transfer $\frac{\partial \theta}{\partial y}$, temperature ($\theta$), skin friction coefficient (C_f), and velocity (U) of the fluid numerically and graphically.

Our analysis shows that:

i) Boosting the value of the Prandtl number (Pr)

minimized the frictional drag coefficient and elevated the rate of heat transport.

ii) With the augmentation in the transpiration parameter, a gradual increase in the thermal flux and frictional coefficient is observed.

iii) An enhancement in the transpiration parameter results in escalated velocity and fluid temperature due to suction.

iv) It is also noted that elevated values of injection accelerate the velocity and thermal characteristics of a fluid. For a diverse range of Prandtl numbers ($\mathrm{Pr} = 0.1, 0.71, 7.0$), distinct fluids (water, air, and oil) showed the same pattern.

Nomenclature

Roman Letters		
x	Coordinate adjacent to the surface	$[m]$
y	Coordinate normal to the surface	$[m]$
$\tilde{u}$	Vertical velocity component	$[\mathrm{ms}^{-1}]$
$\tilde{v}$	Horizontal velocity component	$[\mathrm{ms}^{-1}]$
T	Temperature of fluid	[K]
T_w	Temperature of permeable surface	[K]
T_∞	Free stream temperature	[K]
u	Non-dimensional vertical velocity component	
v	Non-dimensional horizontal velocity component	
U_∞	Ambient fluid velocity	$[\mathrm{ms}^{-1}]$
C_p	Fluid-specific heat	$[\mathrm{Jkg}^{-1}\mathrm{K}^{-1}]$
k_f	Conduction coefficient of fluid	[W/mK]
k_{bf}	Conduction coefficient of base fluid	
k_{hnf}	Conduction coefficient of hybrid nanofluid	[W/mK]
V_o	Permeability of the surface	
Re	Reynolds number	
Pr	Prandtl number	
Greek Letters		
α	Thermal diffusivity	$[\mathrm{m}^2\mathrm{s}^{-1}]$
ξ	Dimensionless transpiration parameter	
θ	Primitive non-dimensional temperature	
ν_f	Kinematic viscosity of the fluid	$[\mathrm{m}^2\mathrm{s}^{-1}]$
μ_f	Fluid's dynamic viscosity	$[\mathrm{kgm}^{-1}\mathrm{s}^{-1}]$
ρ_f	Density of the fluid	$[\mathrm{kgm}^{-3}]$
ρ_∞	Free stream density	$[\mathrm{kgm}^{-3}]$
β_{hnf}	Volumetric expansion coefficient (hybrid nanofluid)	$[\mathrm{K}^{-1}]$
ν_{hnf}	Kinematic viscosity of hybrid nanofluid	$[\mathrm{m}^2\mathrm{s}^{-1}]$
μ_{hnf}	Dynamic viscosity of hybrid nanofluid	$[\mathrm{kgm}^{-1}\mathrm{s}^{-1}]$
ρ_{hnf}	Density of the hybrid nanofluid	$[\mathrm{kgm}^{-3}]$

Data Availability Statement

Data will be made available on request.

Funding

This work was supported without any funding.

Conflicts of Interest

The authors declare no conflicts of interest.

Ethical Approval and Consent to Participate

Not applicable.

References

[1] Clarke, J. F. & Riley, N. (1975). Natural convection induced in a gas by the presence of a hot porous horizontal surface. *The Quarterly Journal of Mechanics and Applied Mathematics, 28*(4), 373-396. [CrossRef]

[2] Schlichting, H., Kestin, J. & Street, R. L. (1980). *Boundary-layer theory* (7th ed.). McGraw-Hill.

[3] Roganov, P. S., Zabolotsky, V. P., Shishov, E. V. & Leontiev, A. I. (1984). Some aspects of turbulent heat transfer in accelerated flows on permeable surfaces. *International Journal of Heat and Mass Transfer, 27*(8), 1251-1259. [CrossRef]

[4] Chaudhary, M. A., Merkin, J. H. & Pop, I. (1995). Similarity solutions in free convection boundary-layer flows adjacent to vertical permeable surfaces in porous media: II prescribed surface heat flux. *Heat and Mass Transfer, 30*(5), 341-347. [CrossRef]

[5] Eastman, J. A. (1999). *Novel thermal properties of nanostructured materials* (Technical Report ANL/MSD/CP-96711). Argonne National Lab.

[6] Hussain, S., Hossain, M. A. & Wilson, M. (2000). Natural convection flow from a vertical permeable flat plate with variable surface temperature and species concentration. *Engineering Computations, 17*(7), 789-812. [CrossRef]

[7] Yu, S. & Ameel, T. A. (2001). Slip-flow heat transfer in rectangular microchannels. *International Journal of Heat and Mass Transfer, 44*(22), 4225-4234. [CrossRef]

[8] Ali, M. & Al-Yousef, F. (2002). Laminar mixed convection boundary layers induced by a linearly stretching permeable surface. *International Journal of Heat and Mass Transfer, 45*(21), 4241-4250. [CrossRef]

[9] Andersson, H. I. (2002). Slip flow past a stretching surface. *Acta Mechanica, 158*(1-2), 121-125. [CrossRef]

[10] Khanafer, K., Vafai, K. & Lightstone, M. (2003). Buoyancy-driven heat transfer enhancement in a two-dimensional enclosure utilizing nanofluids. *International Journal of Heat and Mass Transfer, 46*(19), 3639-3653. [CrossRef]

[11] Maiga, S. E. B., Palm, S. J., Nguyen, C. T., Roy, G. & Galanis, N. (2005). Heat transfer enhancement by using nanofluids in forced convection flows. *International Journal of Heat and Fluid Flow, 26*(4), 530-546. [CrossRef]

[12] Martin, M. J. & Boyd, I. D. (2006). Momentum and heat transfer in a laminar boundary layer with slip flow. *Journal of Thermophysics and Heat Transfer, 20*(4), 710-719. [CrossRef]

[13] Ariel, P. D., Hayat, T. & Asghar, S. (2006). The flow of an elastico-viscous fluid past a stretching sheet with partial slip. *Acta Mechanica, 187*(1-4), 29-35. [CrossRef]

[14] Berg, S., Cense, A. W., Hofman, J. P. & Smits, R. M. M. (2008). Two-phase flow in porous media with slip

boundary condition. *Transport in Porous Media, 74*, 275-292. [CrossRef]

[15] Abu-Nada, E., Masoud, Z. & Hijazi, A. (2008). Natural convection heat transfer enhancement in horizontal concentric annuli using nanofluids. *International Communications in Heat and Mass Transfer, 35*(5), 657-665. [CrossRef]

[16] Ishak, A., Nazar, R. & Pop, I. (2009). The effects of transpiration on the flow and heat transfer over a moving permeable surface in a parallel stream. *Chemical Engineering Journal, 148*(1), 63-67. [CrossRef]

[17] Martin, M. J. & Boyd, I. D. (2010). Falkner-Skan flow over a wedge with slip boundary conditions. *Journal of Thermophysics and Heat Transfer, 24*(2), 263-270. [CrossRef]

[18] Ishak, A. (2010). Similarity solutions for flow and heat transfer over a permeable surface with convective boundary condition. *Applied Mathematics and Computation, 217*(2), 837-842. [CrossRef]

[19] Abu-Nada, E., Masoud, Z., Oztop, H. F. & Campo, A. (2010). Effect of nanofluid variable properties on natural convection in enclosures. *International Journal of Thermal Sciences, 49*(3), 479-491. [CrossRef]

[20] Aziz, A. (2010). Hydrodynamic and thermal slip flow boundary layers over a flat plate with constant heat flux boundary condition. *Communications in Nonlinear Science and Numerical Simulation, 15*(3), 573-580. [CrossRef]

[21] Rahman, M. M., Aziz, A. & Al-Lawatia, M. A. (2010). Heat transfer in micropolar fluid along an inclined permeable plate with variable fluid properties. *International Journal of Thermal Sciences, 49*(6), 993-1002. [CrossRef]

[22] Ashraf, M., Asghar, S., & Hossain, M. A. (2010). Thermal radiation effects on hydromagnetic mixed convection flow along a magnetized vertical porous plate. *Mathematical Problems in Engineering, 2010*, 686594. [CrossRef]

[23] Sheikhzadeh, G. A., Arefmanesh, A., Kheirkhah, M. H. & Abdollahi, R. (2011). Natural convection of Cu-water nanofluid in a cavity with partially active side walls. *European Journal of Mechanics-B/Fluids, 30*(2), 166-176. [CrossRef]

[24] Khan, W. A. & Aziz, A. (2011). Natural convection flow of a nanofluid over a vertical plate with uniform surface heat flux. *International Journal of Thermal Sciences, 50*(7), 1207-1214. [CrossRef]

[25] Su, X. H. & Zheng, L. C. (2011). Approximate solutions to MHD Falkner-Skan flow over permeable wall. *Applied Mathematics and Mechanics, 32*(4), 401-408. [CrossRef]

[26] Suresh, S., Venkitaraj, K. P., Selvakumar, P. & Chandrasekar, M. (2012). Effect of Al_2O_3-Cu/water hybrid nanofluid in heat transfer. *Experimental Thermal and Fluid Science, 38*, 54-60. [CrossRef]

[27] Cortell, R. (2012). Heat transfer in a fluid through a porous medium over a permeable stretching surface with thermal radiation and variable thermal conductivity. *The Canadian Journal of Chemical Engineering, 90*(5), 1347-1355. [CrossRef]

[28] Alvarino, P. F., Jabardo, J. S., Arce, A. & Galdo, M. L. (2012). Heat transfer enhancement in nanofluids: A numerical approach. *Journal of Physics: Conference Series, 395*, 012116. [CrossRef]

[29] Ashraf, M., Asghar, S. & Hossain, M. A. (2012). Computational study of combined effects of conduction-radiation and hydromagnetics on natural convection flow past magnetized permeable plate. *Applied Mathematics and Mechanics, 33*(6), 731-748. [CrossRef]

[30] Huminic, G. & Huminic, A. (2012). Application of nanofluids in heat exchangers: A review. *Renewable and Sustainable Energy Reviews, 16*(8), 5625-5638. [CrossRef]

[31] Noghrehabadi, A., Pourrajab, R. & Ghalambaz, M. (2012). Effect of partial slip boundary condition on the flow and heat transfer of nanofluids past stretching sheet prescribed constant wall temperature. *International Journal of Thermal Sciences, 54*, 253-261. [CrossRef]

[32] Ibrahim, W. & Shankar, B. (2013). MHD boundary layer flow and heat transfer of a nanofluid past a permeable stretching sheet with velocity, thermal and solutal slip boundary conditions. *Computers & Fluids, 75*, 1-10. [CrossRef]

[33] Labib, M. N., Nine, M. J., Afrianto, H., Chung, H. & Jeong, H. (2013). Numerical investigation on effect of base fluids and hybrid nanofluid in forced convective heat transfer. *International Journal of Thermal Sciences, 71*, 163-171. [CrossRef]

[34] Abolbashari, M. H., Freidoonimehr, N., Nazari, F. & Rashidi, M. M. (2014). Entropy analysis for an unsteady MHD flow past a stretching permeable surface in nano-fluid. *Powder Technology, 267*, 256-267. [CrossRef]

[35] Mahdi, R. A., Mohammed, H. A., Munisamy, K. M. & Saeid, N. H. (2015). Review of convection heat transfer and fluid flow in porous media with nanofluid. *Renewable and Sustainable Energy Reviews, 41*, 715-734. [CrossRef]

[36] Sarkar, J., Ghosh, P. & Adil, A. (2015). A review on hybrid nanofluids: Recent research, development and applications. *Renewable and Sustainable Energy Reviews, 43*, 164-177. [CrossRef]

[37] Sidik, N. A. C., Adamu, I. M., Jamil, M. M., Kefayati, G. H. R., Mamat, R. & Najafi, G. (2016). Recent progress on hybrid nanofluids in heat transfer applications: A comprehensive review. *International Communications in Heat and Mass Transfer, 78*, 68-79. [CrossRef]

[38] Hussain, A. M. (2017). Thermal performance and thermal properties of hybrid nanofluid laminar flow

in a double pipe heat exchanger. *Experimental Thermal and Fluid Science, 88*, 37-45. [CrossRef]

[39] Kasaeian, A., Daneshazarian, R., Mahian, O., Kolsi, L., Chamkha, A. J., Wongwises, S. & Pop, I. (2017). Nanofluid flow and heat transfer in porous media: A review of the latest developments. *International Journal of Heat and Mass Transfer, 107*, 778-791. [CrossRef]

[40] Fakour, M., Ganji, D. D., Khalili, A. & Bakhshi, A. (2017). Heat transfer in nanofluid MHD flow in a channel with permeable walls. *Heat Transfer Research, 48*(3), 209-222. [CrossRef]

[41] Sundar, L. S., Sharma, K. V., Singh, M. K. & Sousa, A. C. M. (2017). Hybrid nanofluids preparation, thermal properties, heat transfer and friction factor—A review. *Renewable and Sustainable Energy Reviews, 68*, 185-198. [CrossRef]

[42] Yarmand, H., Zulkifli, N. W. B. M., Gharehkhani, S., Shirazi, S. F. S., Alrashed, A. A., Ali, M. A. B. & Kazi, S. N. (2017). Convective heat transfer enhancement with graphene nano platelet/platinum hybrid nanofluid. *International Communications in Heat and Mass Transfer, 88*, 120-125. [CrossRef]

[43] Bhattad, A., Sarkar, J. & Ghosh, P. (2018). Discrete phase numerical model and experimental study of hybrid nanofluid heat transfer and pressure drop in plate heat exchanger. *International Communications in Heat and Mass Transfer, 91*, 262-273. [CrossRef]

[44] Minea, A. A. & Moldoveanu, M. G. (2018). Overview of hybrid nanofluids development and benefits. *Journal of Engineering Thermophysics, 27*, 507-514. [CrossRef]

[45] Aly, E. H. & Pop, I. (2019). MHD flow and heat transfer over a permeable stretching/shrinking sheet in a hybrid nanofluid with a convective boundary condition. *International Journal of Numerical Methods for Heat & Fluid Flow, 29*(9), 3012-3038. [CrossRef]

[46] Kumar, K. A., Sugunamma, V., Sandeep, N. & Mustafa, M. (2019). Simultaneous solutions for first order and second order slips on micropolar fluid flow across a convective surface in the presence of Lorentz force and variable heat source/sink. *Scientific Reports, 9*(1), 14706. [CrossRef]

[47] Sidik, N. A. C., Adamu, I. M. & Jamil, M. M. (2019). Preparation methods and thermal performance of hybrid nanofluids. *Journal of Advanced Research in Materials Science, 56*(1), 1-10.

[48] Babar, H. & Ali, H. M. (2019). Towards hybrid nanofluids: Preparation, thermophysical properties, applications, and challenges. *Journal of Molecular Liquids, 281*, 598-633. [CrossRef]

[49] Manjunatha, S., Kuttan, B. A., Jayanthi, S., Chamkha, A. & Gireesha, B. J. (2019). Heat transfer enhancement in the boundary layer flow of hybrid nanofluids due to variable viscosity and natural convection. *Heliyon, 5*(4), e01469. [CrossRef]

[50] Ashraf, M., Khan, A. & Gorla, R. S. R. (2019). Natural convection boundary layer flow of nanofluids around different stations of the sphere and into the plume above the sphere. *Heat Transfer-Asian Research, 48*(3), 1127-1148. [CrossRef]

[51] Shafiq, A., Rasool, G. & Khalique, C. M. (2020). Significance of thermal slip and convective boundary conditions in three dimensional rotating Darcy-Forchheimer nanofluid flow. *Symmetry, 12*(5), 741. [CrossRef]

[52] Roy, N. C. & Pop, I. (2020). Flow and heat transfer of a second-grade hybrid nanofluid over a permeable stretching/shrinking sheet. *The European Physical Journal Plus, 135*(9), 768. [CrossRef]

[53] Waini, I., Ishak, A.& Pop, I. (2020). MHD flow and heat transfer of a hybrid nanofluid past a permeable stretching/shrinking wedge. *Applied Mathematics and Mechanics, 41*(3), 507-520. [CrossRef]

[54] Jeelani, M. B. & Abbas, A. (2023). Al_2O_3-Cu ethylene glycol-based magnetohydrodynamic non-Newtonian Maxwell hybrid nano-fluid flow with suction effects in a porous space: Energy saving by solar radiation. *Symmetry, 15*(9), 1794. [CrossRef]

[55] Bhattad, A., Atgur, V., Rao, B. N., Banapurmath, N. R., Khan, T. M. Y., Vadlamudi, C. & Ayachit, N. H. (2023). Review on Mono and Hybrid Nanofluids: Preparation, Properties, Investigation, and Applications in IC Engines and Heat Transfer. *Energies, 16*(7), 3189. [CrossRef]



Uzma Ahmad received the PhD. degree in Mathematics from University of Sargodha, Pakistan, in 2021. Her research interests include environmental heat transfer and climate change, heat and mass transfer, magnetrohydrodynamics and analysis of heat and fluid flow in the presence of catalytic chemical reaction. She served as a lecturer at University of Sargodha since 2012. Now appointed as assistant professor in 2024. (Email: uzma.ahmad@uos.edu.pk)



Kainat Jafri received the MPhil degree in Mathematics from University of Sargodha, Sargodha, Pakistan, in 2024. (Email: kainatjafri44@gmail.com)